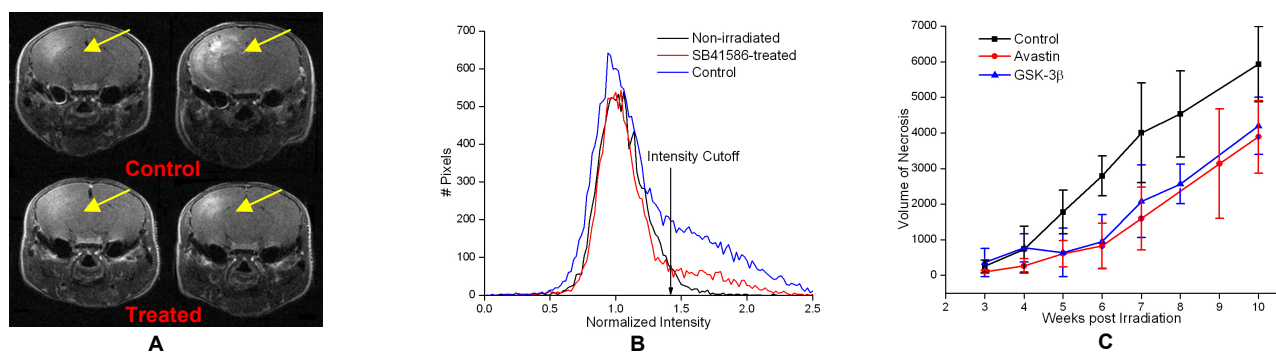


## MRI Describes Mitigation of Radiation Necrosis

Xiaoyu Jiang<sup>1</sup>, John A Engelbach<sup>2</sup>, Jeremy Cates<sup>3</sup>, Dinesh K Thotala<sup>3</sup>, Robert E Drzymala<sup>3</sup>, Dennis E Hallahan<sup>3</sup>, Joseph JH Ackerman<sup>2</sup>, and Joel R Garbow<sup>2</sup>  
<sup>1</sup>Chemistry, Washington University in St. Louis, St. Louis, MO, United States, <sup>2</sup>Radiology, Washington University in St. Louis, St. Louis, MO, United States,  
<sup>3</sup>Radiation Oncology, Washington University in St. Louis, St. Louis, MO, United States

**BACKGROUND AND PURPOSE:** Radiation necrosis is a severe, but late occurring, type of injury to normal tissue, within and surrounding a radiation treatment field. Radiation necrosis is difficult to identify by *in vivo* imaging methods and treatment options are limited. It has been suggested that radiation necrosis results from increases in vascular permeability in brain parenchyma following radiation exposure [1]. Therefore, repair of “leaky” capillaries may delay or prevent the subsequent development and progress of radiation necrosis [2]. Recent reports suggest bevacizumab (Avastin), an anti-angiogenic therapy initially approved for the treatment of metastatic colon cancer and later for other metastatic cancers, may substantially decrease the effects of radiation necrosis [2]. However, to date, there have been no controlled trials of bevacizumab in the treatment of patients with radiation necrosis. It has also been suggested that late time-to-onset radiation necrosis results from acute vascular (endothelial) apoptosis caused by the radiation. Direct over-expression of wild-type GSK-3 $\beta$ , a serine/threonine kinase that is responsible for both cell death and cell survival, is known to induce apoptosis in various cell types in culture. Specific inhibitors of GSK-3 $\beta$  ameliorate this apoptotic process [4]. Recently, an innovative mouse model of radiation necrosis was developed in our laboratory [3] that accurately recapitulates the classic histologic features of radiation necrosis. This mouse model can serve as a robust platform for prospective mitigation study. The purpose of this study was to measure the ability of bevacizumab and SB415286, an inhibitor of GSK-3 $\beta$ , to mitigate radiation necrosis in mouse brain following high-dose radiation treatment. **METHODS:** Three cohorts of mice were irradiated with the Leksell Gamma Knife Perfexion (Elekta; Stockholm, Sweden), a state-of-the-art unit used for stereotactic irradiation of patients with benign and malignant brain tumors. All mice were irradiated with a single 60-Gy dose (50% isodose) of Gamma Knife radiation. In this mouse model, radiation necrosis routinely begins to develop 3 - 4 weeks post irradiation. Mouse cohort #1 was an untreated control; cohort #2 received GSK-3 $\beta$  inhibitor SB415286 (1 mg/kg, daily) from 4 weeks to 7 weeks post irradiation; cohort #3 received bevacizumab (10 mg/kg, twice weekly) from 4 weeks to 10 weeks post irradiation. Mice were imaged weekly, beginning 3 weeks post irradiation using an Agilent/Varian DirectDrive 4.7-T small-animal MR scanner, equipped with Agilent/Magnex self-shielded gradients and high-performance gradient power amplifiers (International Electric Company). All the mice were sacrificed following the last imaging session at 10 weeks post irradiation. **RESULTS:** Slices from representative contrast-enhanced, T1-weighted spin-echo images of control (top) and SB415286-treated (bottom) mice, collected 4 and 8 weeks post-irradiation, are shown in Figure 1(A). At 8 weeks post irradiation, regions of hyperintensity (yellow arrows) associated with radiation necrosis are much larger in the control mouse than in the inhibitor-treated mouse, indicating that radiation necrosis progresses more rapidly in the control mouse. For each mouse in each cohort, regions of interest were drawn around the entire brain in 10 contiguous image slices, chosen to include the irradiated region, intensity for each region of interest was normalized by the mean intensity of the right brain (unirradiated hemisphere), and histograms of image-pixel intensity were constructed. Figure 1(B) shows representative histograms for irradiated control and SB415286-treated mice, together with the average image-pixel intensity distribution for a cohort (n=3) of non-irradiated mice. For non-irradiated subjects, the intensity distribution histogram is symmetric, with the majority of the pixels being distributed in the intensity range 0.6 – 1.4 about a normalized mean of 1.0. An intensity threshold of 1.4 (Figure 1(B), arrow) was chosen as the cutoff for normal brain tissue. For images of irradiated mice, the number of pixels exceeding this threshold served to measure the volume of radiation necrosis. The average number of hyperintense pixels for cohorts (n=6) of control, inhibitor-treated, and bevacizumab-treated mice are plotted as a function of time post irradiation in Figure 1(C). For the period 4 to 7 weeks, the progression of necrosis in the inhibitor-treated and bevacizumab-treated mice is much slower than for the control mice; differences in necrosis volumes between control and treated mice are statistically significant on weeks 5, and 6 (P<0.05); from weeks 7 to 10, necrosis develops at approximately the same rate (slope of the plot of hyperintense pixels vs. post-irradiation time) as in control animals. For the SB415286-treated mice, this trend is consistent with the treatment period. For the bevacizumab-treated mice, the progression of necrosis was greatly reduced during the early treatment period, but increased significantly during the latter 3 weeks of treatment. **CONCLUSION:** These data demonstrate a significant reduction in the progression of radiation necrosis in mice following administration of either bevacizumab or SB415286, a GSK-3 $\beta$  inhibitor, compared to untreated, irradiated mice. Efforts to optimize dosing schemes and to verify mechanism of action for both SB415286 and bevacizumab, including attempts to understand the development of resistance to bevacizumab treatment, are in progress.



**Figure 1.** (A) Contrast-enhanced T1-weighted images of control mouse (top), and SB415286-treated mouse (bottom), 4 (left) and 8 weeks (right) after Gamma Knife irradiation. (B) Image-pixel intensity histogram for non-irradiated (blue); SB415286-treated, irradiated (red); and DMSO-treated, irradiated (blue) mice; the intensity cutoff used to define hyperintense pixels, corresponding to necrotic tissue, is indicated by the arrow. (C) Average, MRI-defined volumes of radiation necrosis vs. time post-irradiation for cohorts (n=6) of control, SB415286-treated, and bevacizumab-treated mice.

**REFERENCES:** (1) Li YQ, Ballinger JR, et al. Hypoxia in radiation-induced blood-spinal cord barrier breakdown. *Cancer Res* 2001; **61**: 3348-54. (2) Gonzalez J, Kumar AJ, et al. Effect of bevacizumab on radiation necrosis of the brain. *Int J Radiat Oncol Biol Phys* 2007; **67**: 323-6. (3) Jost SC, Hope A, et al. A novel murine model for localized radiation necrosis and its characterization using advanced magnetic resonance imaging. *Int J Radiat Oncol Biol Phys* 2009; **75**: 527-33.; (4) Thotala DK, Hallahan DE, Yazlovitskaya EM. Inhibition of glycogen synthase kinase 3 beta attenuates neurocognitive dysfunction resulting from cranial irradiation. *Cancer Res* 2008; **68**: 5859-68.